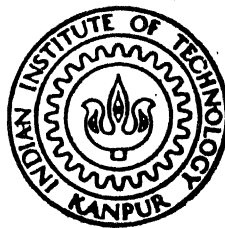# EFFECT OF HEAT TREATMENT ON FRACTURE TOUGHNESS OF A MEDIUM CARBON LOW ALLOY STEEL

By

MANOJ KUMAR JAIN

DEPARTMENT OF METALLURGICAL ENGINEERING

INDIAN INSTITUTE OF TECHNOLOGY, KANPUR

SEPTEMBER, 1988

EFFECT OF HEAT TREATMENT ON FRACTURE TOUGHNESS OF A MEDIUM CARBON LOW ALLOY STEEL

A Thesis Submitted
In Partial Fulfilment of the Requirements
for the Degree of

MASTER OF TECHNOLOGY

By

MANOJ KUMAR JAIN

to the

DEPARTMENT OF METALLURGICAL ENGINEERING

INDIAN INSTITUTE OF TECHNOLOGY, KANPUR

SEPTEMBER, 1988
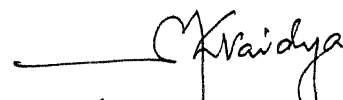
ME- 1988 - M - JAI - EFF

CERTIFICATE

It is certified that this work entitled EFFECT OF HEAT TREATMENT ON FRACTURE TOUGHNESS OF A MEDIUM CARBON LOW ALLOY STEEL has been carried out by Mr. Manoj Kumar Jain under my supervision and the same has not been submitted elsewhere for a degree.

(M.L. Vaidya)
Professor and Head
Deptt. of Metallurgical Engg
I.I.T. Kanpur.

ACKNOWLEDGEMENT

I take this opportunity to express my profound gratitude and appreciation to Dr. M.L. Vaidya for his inspiring and valuable guidance and persistent encouragement provided to me at all stages of this work. It was indeed a pleasure to work under him.

I am also indebted to Dr. A.K. Patwardhan, Head, Department of Metallurgical Engineering, University of Roorkee, Roorkee for allowing me to use the facility of scanning electron microscope and providing all the necessary help.

Thanks are also due to Mr. H.C. Srivastava, Mr.B.K. Jain, Mr. K.P. Mukherji and other staff of Metallurgical Engineering Department for their help and co-operation.

Thanks to Mr. R.K. Jain for his excellent and flawless typing.

Last but not the least thanks are due to all my friends who made my stay at this campus pleasurable and memorable one.

(MANOJ KUMAR JAIN)

CONTENTS

ABSTRACT

A commercially important medium carbon low alloy steel (composition close to AISI 4135) has been subjected to a range of tempering temperature after oil quenching from $870^\circ C$. Impact toughness and fracture toughness(K_{IC}) have been studied over a range of tempering temperatures of $200^\circ C$ to $450^\circ C$. These have been supplemented by hardness, yield strength and tensile strength measurements over the same range of tempering temperatures. Microstructural and Fractographic studies have been carried out to understand the variations in the toughness values. The significant findings are: Impact toughness initially increases to a value of 106.8 joules, then decreases to a minimum value of 29.4 joules and finally increases to 69.6 joules, K_{IC} increases from 53.5 MPa$\sqrt{m}$ to 115.0 MPa$\sqrt{m}$ in the range of temperatures where impact toughness decreases. Other mechanical properties decrease continuously with increasing tempering temperature. The difference in the impact toughness and K_{IC} is explained in terms of strain rate effect on properties.

<u>LIST OF TABLES</u>   <u>Page No.</u>

LIST OF FIGURES

CHAPTER-I

INTRODUCTION

Low alloy (< 5% alloying elements content) medium carbon
(between 0.3 to 0.5% carbon) steels are used extensively
in heat-treated condition in applications demanding high
strength (> 150 ksi). Generally, higher the strength
greater is the tendency of brittle fracture. Therefore
it is desirable to combine strength with toughness
(resistance to brittle fracture) in these steels with
proper heat-treatment procedures. Whereas the role of
structure on the strength is well understood, there are
large problems in understanding toughness in terms of the
structure. One reason may be that there exist a lot of
different toughness criteria- e.g., ductility in the tensile
test, impact toughness, fracture toughness etc.

1.1 Impact Toughness and Fracture Toughness:

Impact tests are used to indicate the toughness of a
material under shock loading conditions. It measures the
energy necessary to fracture a standard notched-bar by an
impulse load and as such is an indication of the notch
toughness of a material under shock loading. A large number
of notched-bar test specimens of different design have been
used by investigators of the brittle fracture of metals. Two
classes of specimens have been standardized[1] for notched-impact

testing, Charpy bar specimens which are used most commonly
and the Izod specimen, which is used rarely today. This type
of test will detect differences between materials which are
not observable in a tension test. The chief engineering use
of the Charpy test is in selecting materials which are
resistant to brittle fracture by means of transition-temperature
curves. When conducted over a series of temperatures, it can
be used to uncover any temperature-dependent transition from
ductility to brittleness.

The test is frequently used for quality control and
material acceptance purposes. The chief difficulty is that
the results of the Charpy test are difficult to use in design.
The fracture energy measured by the Charpy test is only a
relative energy and can not be used directly in design
equations. Since there is no measurement in terms of stress
level, it is difficult to correlate C_V, the energy required
for fracture, with service performance. Moreover, there is
no correlation of Charpy data with flaw size. In addition,
the tests are subject to considerable scatter. Most of this
scatter is due to local variations in the properties of the
steel, while some is due to difficulties in preparing perfectly
reproducible notches. Both notch shape and depth are critical
variables, as is the proper placement of the specimen in the
impact machine. Furthermore, there is no general agreement
on the interpretation or significance of results obtained with

this type of test.

The fracture toughness, the toughness in the statically loaded condition in presence of sharp fatigue crack is a basic material property, and is gaining wider acceptance to the designers for designing complicated structures and components and evaluating structural reliability for critical applications, for preliminary selection of alloys for particular uses and to the failure analyst for analysis of failure and its prevention. A properly determined value of K_{IC}, plane-strain fracture toughness, represents the fracture toughness of the material independent of crack length, geometry, or loading system. It is a material property in the same sense that yield strength is a material property. The basic equation for fracture toughness is:

$$K_{IC} = \sigma_f \sqrt{\pi a}$$

where σ_f = fracture stress

a = $\frac{1}{2}$ x crack length

K_{IC} has the dimensions of $MPa\sqrt{m}$

If the material is selected, K_{IC} is fixed. If we allow for the presence of a known size of crack, then the design stress is fixed. On the other hand, if the stress level is known, the maximum allowable flaw size can be determined. These trade offs between fracture toughness, allowable stress, and crack size are illustrated in Fig. 1.1[2].

Reliable and efficient design of an engineering component owes
heavily to the development of high fracture toughness in the
material of which the component is made of. This parameter
has been recognized to be structure-sensitive and depends on
the heat treatment conditions. In the case of steels, to
obtain a best combination of mechanical properties, quenching
and tempering is the most important and most commonly used
type of heat treatment.

1.2 Quench Hardening and Tempering Treatment:

Steels that have undergone a simple hardening quench
are usually mixtures of austenite and martensite, with the
latter constituent predominating. These steels are of little
useful value because

(i)   Both of these structures are unstable and slowly
       decompose, at least in part, if left at room temperature.
       As a result of these changes, hardened steel objects
       undergo dimensional changes as a function of time when
       left at room temperature.

(ii)   A structure which is almost completely martensite is
       extremely brittle.

(iii) As a result of the above two factors steel is very liable
       to develop quench cracks if aged at room temperature.

To improve the mechanical properties of quenched steels a
simple heat treatment called tempering is almost always used.
In this treatment, the temperature of the steel is raised to a

value below the eutectoid temperature, held there for a fixed length of time after which the steel is cooled again to room temperature. The object of tempering is to relieve the internal stresses of a quenched steel, to reduce the hardness and to obtain greater ductility and toughness than associated with the high hardness of the quenched steel.

1.3 **Aim of the Present Investigation:**

The material used in this investigation is a medium carbon (0.33 to 0.37%)low alloy steel of given composition close to the steel composition AISI 4135. This type of medium carbon low alloy steel is widely used in quenched and tempered condition for various structural applications such as chain links for earthmoving equipments etc. The steel is currently used after tempering at: 450°C. The present study has been carried out keeping in view the following aims:

(i) The plane-strain fracture toughness, K_{IC}' values for this steel in quenched and tempered condition and at differen tempering temperatures are not available in literature. The significance of plane-strain fracture toughness testing as compared to impact testing has already been discussed.

(ii) To select a suitable tempering temperature for this steel especially in the lower tempering temperature range at which a good combination of fracture toughness with other mechanical properties such as impact toughness, strength etc. can be obtained. It will result into cutting down

the energy consumption and time required for the whole operation as steel will have to be heated to a lower temperature. High tempering temperature not only results in higher energy consumption and processing time but also increased softening and lowering of strength of steel.

(iii) To study the fracture behaviour of the present steel under different loading conditions as encountered in K_{IC} testing and Charpy impact testing with varying tempering temperature if both means of toughness evaluation are similarly sensitive to tempering temperature.

The present work is planned to study the mechanical properties like fracture toughness (using a three-point bend specimen), impact toughness (using a Charpy V-notch specimen), hardness and tensile behavior of steel quenched and tempered at different temperatures.

CHAPTER-II

LITERATURE REVIEW

This chapter presents a brief introduction to the concept
of FRACTURE TOUGHNESS and its evaluation followed by a
review of factors affecting fracture toughness of materials
in general. Finally, a critical review of literature on
fracture toughness studies in heat-treated steels and the
associated phenomena of, Temper Embrittlement(TE) and
Tempered Martensite Embrittlement(TME) is presented.

2.1 Concept of Fracture Toughness[2]:

The theoretical fracture strength for a brittle
elastic solid is given by

$$\sigma_{max} = (\frac{E\gamma_s}{a_o})^{1/2}$$

E = modulus of elasticity

γ_s =surface energy of the fracture surface per unit area

a_o =equilibrium interatomic spacing

Engineering materials typically have fracture stresses that
are 10 to 1000 times lower than the theoretical value. This
leads to the conclusions that flaws or cracks are responsible
for this discrepency. Griffith showed that fracture stress
in the presence of a crack is

$$\sigma_f = (\frac{2E\gamma_s}{\pi a})^{1/2} \qquad\qquad a = 1/2 \text{ x crack length}$$

Metals which fail in a completely brittle manner also undergo some plastic deformation prior to fracture. Therefore, Griffith's equation for the fracture stress does not apply for metals. Orowan suggested that[1]

$$\sigma_f = \left(\frac{2E(\gamma_s + \gamma_p)}{\pi a}\right)^{1/2}$$

γ_p = plastic work required to extend the crack wall

$$\left(\frac{E\gamma_p}{a}\right)^{1/2} \qquad (\gamma_p >> \gamma_s)$$

It was further modified by Irwin as γ_p is difficult to measure.

$$\sigma_f = \left(\frac{EG_c}{\pi a}\right)^{1/2}$$

G_c corresponds to a critical value of $G(= \frac{\pi a \sigma^2}{E})$, the crack extension force. G also may be considered the strain-energy release rate, i.e., the rate of transfer of energy from the elastic stress field of the cracked structure to the inelastic process of crack extension. The critical value of G which makes the crack propagate to fracture G_c is called the fracture toughness of the material. Irwin pointed out that the local stresses, near a crack depend on the product of the nominal stress σ and the square root of half flaw length.

He called this relationship the stress intensity or K,

where for a sharp elastic crack in an infinitely wide plate,

K is defined as

$$K = \sigma\sqrt{\pi a}$$ The units of K are MPa$\sqrt{m}$

In dealing with the stress intensity factor there are several

modes of deformation that could be applied to the crack.

These have been standardized as Mode I, Mode II and Mode III.

Mode I, i.e., the crack-opening mode loading is the most

important situation. This is the usual mode for fracture-

toughness tests and a critical value of stress intensity

for this mode would be designated K_{IC}. There are two extreme

cases for mode I loading, plane-stress and plane-strain.

The plane-strain condition represents the more severe stress

state and the values of K_{IC} are lower than for plane-stress

specimen. Plane strain values of critical stress intensity

factor K_{IC} are valid material properties, independent of

specimen thickness, to describe the fracture toughness of

materials.

2.2 Evaluation of Plane Strain Fracture Toughness (K_{IC}):

Plane strain fracture toughness   testing has been

standardized by ASTM, Designation E399-707[3]. A variety of

test specimens have been proposed for measuring K_{IC} plane

strain fracture toughness. The compact tension specimen and

the three-point loaded bend specimen have been standardized by ASTM. These are shown in Fig. 2.1[2]. Fig. 2.2[2] shows how the fracture stress varies with specimen thickness B. Once the specimen has the critical thickness for the toughness of the material, the fracture stress is constant with increasing specimen thickness. The minimum thickness to achieve plane-strain conditions and valid K_{IC} measurements is

$$B = 2.5[\frac{K_{IC}}{\sigma_o}]^2 \qquad \sigma_o = \text{yield strength of the material}$$

After the notch is machined in the specimen, the sharpest possible crack is produced at the notch root by fatiguing the specimen. The test is carried out in a testing machine which provides for a continuous autographic record of load P and relative displacement across the open end of the notch (Proportional to crack displacement). A value P_Q at which unsteady crack propagation takes place is determined from the load-displacement curve and is used to calculate a conditional value of fracture toughness denoted by K_Q.

For the bend specimen:

$$K_Q = \frac{P_Q S}{BW^{3/2}} f(a/W)$$

B= specimen thickness

w= specimen width

S= Span

a= initial crack length including both the notch and the fatigue crack.

$$f(\tfrac{a}{W})=[2.9(\tfrac{a}{W})^{1/2}-4.6(\tfrac{a}{W})^{3/2}+21.8(\tfrac{a}{W})^{5/2}-37.6(\tfrac{a}{W})^{7/2}+38.7(\tfrac{a}{W})^{9/2}]$$

Next, the factor $2.5(\tfrac{K_Q}{\sigma_o})^2$ is calculated. If this quantity is less than both the thickness and crack length of the specimen, then K_Q is equal to K_{IC} and the test is valid. Otherwise it is necessary to use a thicker specimen to determine K_{IC}. The measured value of K_Q can be used to estimate the new specimen thickness.

2.3 Factors Affecting Fracture Toughness of Materials:

Fracture Toughness is a measure of material resistance to fast crack propagation under external loading. It is a highly structure sensitive property. It depends on

(i) Nature of phases present in a material, their volume fractions and morphologies.

(ii) Grain size of the matrix phase.

(iii) Texture

(iv) Inclusions

(v) Impurity Contents

(vi) Temperature and Strain Rate

2.3.1 Nature of Phases Present in a Material:

Phases in which dislocation motion is very difficult exhibit low fracture toughness values. These are essentially

brittle phases and the fracture toughness of these phases
depend mainly on their surface energy values. Phase, where
dislocation motion is rather easy, exhibit higher fracture
toughness values. Dislocation motion and their interactions
play a major role in these materials (ductile phases)[4].

In materials which contain both brittle and ductile
phases, fracture toughness values depend on volume fraction
of these phases and their morphologies. As the volume fraction
of ductile phases increases fracture toughness tends to
increase, provided the morphology of the brittle phases is
proper.

Generally lammelar, disc shaped or lenticular shaped
brittle phases lower fracture toughness of the materials.
Spheroidal[4] or oblate spheroidal shapes of the brittle phases
enhance fracture toughness values. These shapes very much
depend on processing history of a material.

Distribution of phases is another morphological feature
which affects the fracture toughness of a material. If the
brittle phases are distributed along grain boundaries[2] of the
material, fracture toughness is adversely affected. For
better toughness values, the brittle phases should be distributed
within the grains and in finely divided form.

There is one more aspect of the phases when present in
a manner in a material and that is the coherency[2] between the

matrix phase and the distributed phase. If there is
a complete coherency between the phases, fracture toughness
tends to be lower as compared that of an incoherent situation.

2.3.2 Grain Size Effect:

In single phase materials fracture toughness is higher
for fine grained materials. Grain boundaries offer greater
resistance to crack propagation and hence the greater fracture
toughness in materials containing higher density of the grain
boundaries.

In multiphase materials it is the grain size of the
matrix phase which controls the fracture toughness values.
But there is no clear trend established. The complexity in
the relationship between K_{IC} and grain size has been presented
by Schwalbe[5].

2.3.3 Textural Effects:

The importance of texture in fracture toughness
studies becomes evident from the findings of Johnson and
Radon[6]. Working with an Al-4.1 Cu alloy, they found that the
fracture toughness, K_{IC} value of a hot-rolled plate is
reduced along the transverse direction to one-third to two-
thirds of the value for the longitudinal direction (rolling
direction).

2.3.4 Effect of Inclusions:

Low tensile strength and weak interfacial bonding of
inclusions are the reasons for void nucleation at low strains[7].

These voids act like small cracks accompanied by highly localized stresses and strains depending on content, size, shape, distance and orientation to deformation axis. Whilst the material strength is not influenced by inclusions, toughness and ductility are very sensitive parameters for impurities. Marked reductions of toughness and ductility are the result, if large inclusions are present in the material .

2.3.5 Effect of Impurity Contents:

The presence of impurity elements results in decrease in fracture toughness of materials. The embrittling elements segregate at grain boundaries. These segregated solute atoms decrease the grain boundary surface energy, thus providing an easy propagation path for a crack leading to intergranular embrittlement[2].

2.3.6 Temperature and Strain Rate Effects:

For a given metallurgical structure toughness increases with increasing temperature and with decreasing strain rate or rate of loading[2].

2.4 Observations on Heat Treatable Steels:

In steels under different heat treatment conditions, different structures are obtained such as Pearlite, Bainite, Martensite and Retained Austenite. There are certain common impurities in steels viz., O,H,N,P,S, Bi, Sb, Sn and As. Steels also contain variety of non-metallic inclusions such as MnS, MnO, Al_2O_3 and SiO_2 etc.

2.4.1   Effect of Various Structures on Fracture Toughness:

2.4.1   (a) Effect of Pearlite and Bainite Structures:

The effect of the percentage of pearlite or bainite on fracture toughness of HF-1 steel has been studied by Weiner et al[8]. They found that, as the percentage of pearlite increased, the fracture toughness at room temperature decreased. However, the presence of bainite, even in rather small percentages (0%-10%), causes a catastrophic decrease in fracture toughness. For bainite contents higher than 10%, the fracture toughness remained nearly unaffected.

2.4.1   (b) Effect of Martensitic Structure:

Martensite in carbon steels can form by two reactions. One gives a structure known as Lath Martensite, the other is a Lenticular Martensite that is internally twinned. The lath martensite is characterized by a high internal dislocation density of the order of 10^{11} to $10^{12}/cm^2$. The twinned martensite normally does not contain a high density of dislocations. It has been found that twins lower fracture toughness and increase strength[9]. Padmanabhan and Wood[10] in their studies on 300M steel observed that the K_{IC} variation for different heat treatments was consistent with the twin density variation. Other significant factors which govern K_{IC} are the lath width and packet size. The same authors observed that decreasing lath width and packet diameter elevates σ_f and, hence , ε_f and thus K_{IC}.

2.4.1 (c) Retained Austenite Effect:

Retained austenite (f.c.c.) has a positive effect on fracture toughness. Many workers[11,12,13] have found that the fracture toughness increased with increasing amounts of retained austenite. The retained austenite phase being softer and tougher than the martensite plates serves as crack blunter. The crack while passing through the austenite phase gets blunted and requires more and more energy for its propagation. This might lead to the crack arresting and improved K_{IC} values[13]. Since austenite is f.c.c., cleavage fracture is not favoured[14]. Thus increase in toughness on increasing the relative amount of retained austenite may be accounted for.

But Harn and Ritchie[15] while studying the phenomenon of tempered martensite embrittlement on two commercially important AISI 4340 and 300M steels have strongly questioned the beneficial role of retained austenite on the toughness of alloy steels. According to them before claiming any beneficial role of retained austenite its thermal and mechanical stability should be defined.

"Thermal Stability" means variation of percentage of austenite in unstressed (prior to loading) structures with respect to tempering temperature. Retained austenite continuously decreases with increasing tempering temperature. "Mechanical Stability" means variation of austenite percentage after strain

with respect to tempering temperature. They found that the mechanical stability of austenite seen by comparing unstressed levels with those after 0.2 and 2.0 percent strain, is somewhat different. Austenite present in the untempered structure is extremely unstable. The mechanical stability increases first with tempering temperature but it becomes mechanically destabilized again at tempering temperature which corresponds to where tempered martensite embrittlement occurs. According to them austenite is retained as interlath films in as quenched structures. This high carbon austenite on lath boundaries can then act as a primary source for the precipitation and growth of embrittling carbide films at austenite-martensite lath interfaces. Once the carbides form, the austenite becomes depleted in carbon, and accordingly becomes mechanically unstable. On deformation, the unstable austenite transforms to leave an embrittling film of untempered martensite on lath boundaries. If the retained austenite is large enough the fracture mode is found to be interlath cleavage. Therefore according to them thermally and mechanically unstable austenite is not beneficial at all. They also raised the question whether stable retained austenite can be beneficial to toughness. If it is so then it is with strength loss.

2.4.1 (d) <u>Effect of Austenitizing Temperature</u>:

Ritchie and Horn[16] studied the influence of austenitizing temperature on the fracture toughness of

commercial AISI-SAE 4340 steel. They found that the plane
strain fracture toughness K_{IC} increased as the austenitizing
temp was raised. Fig. 2.3 depicts their results for untempered
and tempered (at $200^{\circ}C$) AISI-SAE 4340 steel. Similar
observations were made by Kumar and Seal[13] on two commercially
important low alloy steels En16 and En19. A two fold
improvement in K_{IC} was noticed for En19 steel by increasing
austenitizing temperature from $850^{\circ}C$ to $1050^{\circ}C$. They
attributed the improvement in static fracture toughness values,
K_{IC} with austenitizing temperatures to a number of factors.

The increased austenitizing temperature gives rise to
increased amount of retained austenite in the matrix. They
explained the increase in fracture toughness due to beneficial
effects of retained austenite as discussed earlier. The
removal of undissolved carbides or second phase particles
from the matrix at higher soaking temperatures might also
influence the K_{IC} values. The carbides|second phase particles
are considered to be the primary initiators for voids/cracks
due to localization of shear bands.

Charpy impact toughness values were found first to
decrease and then increase as austenitizing temperature was
raised. So, no direct relationship between impact toughness
and austenitizing temperature was found. Kumar and Seal[13]
attributed the insensitivity of Charpy values to the notch

bluntness and dynamic loading. A small change in microstructure due to small variation in austenitizing temperature is quite unlikely to be reflected on dynamic toughness. However, in literature[17] a reduction in dynamic toughness values has been reported for Ni-Cr-Mo, Ni-Cr-Mo-V, 4340 and 300M steels with increased austenitizing temperature. The contradictory behavior can be explained in terms of strain rate effect, notch acquity and shear lip effects etc.[18]. It is to be noted that the Charpy values give relative toughness and significant scatter in results. Accordingly, the observed trend has to be interpreted with caution.

2.4.2 Impurity Effects on Fracture Toughness:

It has been found that the presence of impurity elements has a deleterious effect on fracture toughness of steels. The Chief embrittling elements are O,H,N,P,S,Si,Bi,Sb, Sn and As. The severity of embrittlement increases with the concentration of these impurities. Musiol and Brook[11] concluded that lowering the oxygen content of the same steel results in an improvement in fracture toughness. Schwalbe[5] presented data on the influence of sulfur on fracture toughness of 0.45C-Ni-Cr-Mo steels. Changing the sulfur content from 80 to 490 PPM caused a decrease in the fracture toughness K_{IC} value of 25 MPa$\sqrt{m}$. Materkowski and Krauss[19] studied the effect of P on fracture toughness of 4340 steel with low (0.003 wt PCt) and

nominal (0.03 wt Pct) amounts of P. No change in hardness values was found in low P and high P steels. But the impact energy of the low P steel was observed higher than that of the high P steel at all tempering temperatures, Fig. 2.4. P lowers the absorbed energy and raises the transition temperature. In the case of high P steel K_{IC} values were also lower than low P steel. Intergranular fracture has been observed in such cases.

2.4.3 Effect of Non-Metallic Inclusions:

Non-metallic inclusions have deleterious effect on fracture toughness of steels. As a first hypothesis it can be assumed that fracture occurs, if the fracture strain of tempered martensite is exceeded at any point of the specimen, at the stress conditions given in this place. A model, developed by Fujita et al[20,21] predicts the following relationship:

$$\varepsilon_f = constant.1./1^{1/(1+n)} \qquad constant = (\frac{K_{IC}}{\pi\sigma_y})^{1/(1+n)}$$

l = length of the inclusion

n = strain-hardening exponent

which shows the importance of matrix toughness, the yield stress, the strain hardening exponent and inclusion length. Steel which has shorter inclusions has the better transverse ductility. Ebner and Maurer[22] while studying the effect of non-metallic inclusions on fracture toughness of a medium carbon low alloy high strength steel observed that oriented inclusions, like MnS, cause anisotropic properties.

Slatcher and Knott[23] in their investigations on tempered martensitic alloy steels observed the effect of two predominant inclusion types, MnS and 3MnO. Al_2O_3. $3SiO_2$ and concluded that inclusion content of these steels does not have a marked effect on their toughness., They deduced that it is tempered martensitic microstructure which plays the most important role in determining the fracture toughness of such steels.

2.5 K_{IC} and Other Mechanical Properties of Quenched and Tempered Steels:

In order to understand fracture toughness and other mechanical properties of quenched and tempered steels, it is necessary to summarize first, the microstructural changes that occur during tempering of steels.

2.5.1   Changes that Occur During Tempering Treatment[24]:

It is common practice to subdivide the reactions that occur during tempering into three stages based on tempering temperature.

The reactions during the first stage of tempering occur at rates that can be measured in the temperature interval between room temperature and approximately 200°C. The first principal effect is some of the carbon atoms diffuse to and collect around the dislocations in the lath martensite component of the structure. A carbide is observed to precipitate, which is known as Epsilon(ε) carbide from that fraction of carbon not segregated at the dislocations and lath boundaries, i.e.,

which is present in the normal interstitial sites. Simultaneously
with the precipitation of ε carbide, a low carbon martensite
nucleates separately and grows. The carbon content of this
new phase low carbon martensite is approximately 0.30% and
independent of the original martensite carbon content. The
carbide particles are extremely small in size, as is to be
expected considering the low temperature range at which they
form.

The reactions during the second stage of tempering occur
in the temperature range 100-300°C. Here, the retained
austenite transforms to bainite. At temperatures below 100°C
austenite may be assumed to transform to martensite and not
bainite. The microstructure of the bainite that forms consists
of ferrite and ε carbide while decomposed martensite obtained
in the first stage of tempering has a matrix of low carbon
tetragonal martensite with ε carbide particles.

The reactions in the third stage of tempering occur
at temperatures above 200°C. In these reactions basically
ferrite and cementite form from the reaction products of stages
one and two. Carbon steels in which the structure is essentially
all martensite, a rod-shaped carbide particle can develop between
200 to 250°C. This can be formed at the expense of the carbon
segregated to the dislocations and lath boundaries. The ε
carbide dissolve and the low-carbon martensite loses both its

carbon and tetragonality and becomes ferrite or cubic iron.
At 400°C the rod shaped carbides dissolve and are replaced
by spherical cementite particles. Between 500 and 600°C the
recovery of the dislocations in the lath boundaries occur
resulting in a low-dislocation-density acicular ferrite
structure. On further heating to 600 to 700°C, the acicular
ferrite grains then recrystallize to form an equiaxed ferrite
structure. The end result is an aggregate of equiaxed ferrite
grains containing a large number of spheroidal cementite
particles. Finally the spheroidal carbide particles grow.
Fig. 2.5[22] shows possible types of microstructures depending
on tempering temperature.

Steels having appreciable amounts of carbide forming
elements when tempered below 540°C, alloying elements are
present in the cementite particles in the form of $(Fe,M)_3C$
where M represents any of the substitutional element. However,
when the tempering temperature exceeds 540°C, appreciable
amounts of alloy carbides are precipitated which, in general,
do not conform to the formula $(Fe,M)_3C$. It results in "Secondary
Hardening" of steel which is believed due to coherency[25]. At
low tempering temperatures the rate of diffusion of substitutional
elements is too slow to permit the formation of alloy carbides.
$(Fe, M)_3C$ can form is because the diffusion rate of carbon is
still very large at temperatures below 540°C. Therefore, most
alloying elements in steels tend to increase the resistance of
the steel to softening when it is tempered. Fig. 2.5[26] shows

the effect of Si (non-carbide forming) and Mo (Carbide-forming) on softening characteristics in tempering of a steel.

2.5.2 <u>Mechanical Property Changes</u>:

The microstructural changes that occur during tempering greatly change the mechanical properties of steel . In general, the hardness decreases[24] as temperature and time of tempering both increase. If steel samples contain finite amounts of retained austenite, a rise in hardness is observed just above room temperature as a result of the conversion of retained austenite into martensite or bainite. During the first stage of tempering, while the precipitation of ε carbide undoubtedly contributes a hardening component to the steel, the depletion of carbon from the martensite matrix can be expected to contribute a softening component. The observed hardness, therefore, reflects the result of these two effects. A slight increase in hardness (not due to retained austenite) may be observed in the high carbon steels due to the large amount of ε carbide precipitated. In the early part of third stage, both the solution of ε carbides and the removal of the carbon from the martensite (low-carbon form) should soften the metal. However, at the same time, cementite precipitates contribute a hardening effect when the steel has attained a simple ferrite and cementite structure, further softening results from the growth or coalescence of cementite particles. To attain a given hardness, higher is the tempering temperature, lower

is holding time.

$$\frac{1}{t} = A \ e^{-\frac{Q}{RT}}$$

t = holding time

T = tempering temperature

Q = activation energy for the process

A and R are the constants

A method has also been developed by Crafts and Lamont[27] by which the hardness of a quenched steel after tempering for 2 hours at a particular temperature can be estimated. The correlation between the experimental and calculated results is not perfect but it is satisfactory.

Tensile strength and yield strength also decrease as tempering temperature increases in accordance with the hardness. Ductility as measured in terms of % elongation and % reduction in area increases with tempering temperature. Fig. 2.7[26] shows the influence of tempering temperature on these mechanical properties for one particular steel.

In general, both static as well as dynamic toughness increase as tempering temperature is raised. In medium and high tempering temperatures, carbide precipitates are embedded in a metallic matrix consisting of martensite laths and packets. Recent investigations[22] emphasized the role of carbides in the fracture process, especially their influence on void nucleation and growth. The dominating failure mechanism

depends on shape; plate-like carbides are often breaking, whereas spheres often fail by decohesion of the particle | matrix interface. Fracture surface investigation of specimens indicate either intergranular fracture or transgranular fracture relative to the prior austenitic grain structure. The transgranular fracture[19] may be interlath, i.e., between the parallel martensite units or laths that typically form in low and medium carbon steels or it may be translath, i.e., across the martensite lath rather than between them. Translath fracture is cleavage across the packets of parallel laths, most of which have the same orientation and therefore, the same orientation of their {100} cleavage planes. Carbide spheroidization[22] coincides with a maximum in ductility and toughness. This is effected by both beneficial carbide shape and lower strength caused by a reduction in dislocation density.

2.5.3 Correlation of K_{IC} with other Mechanical Properties:

The fracture toughness decreases as yield strength and tensile strength increases . The inverse relationship was also found between fracture toughness and hardness. Fracture toughness values are directly related with ductility measured in terms of % elongation, % reduction in area and true fracture strain. Kumar and Seal[28] tried to correlate fracture toughness with these mechanical properties mathematically and established some empirical relations for two commercially important En-16 and En-19 steels. The range of toughness and yield strength

values for a variety of alloys at room temperature is shown in Fig. 2.8[2].

Slatcher and Knott[23] while studying the fracture toughness of tempered martensitic alloy steels concluded that the fracture toughness of these steels is inversely correlated with the work hardening rate, which is contrary to what might be expected considering the experimental evidence of other alloy systems[29] and most theoretical predictions.

There has been a lot of controversy in the literature on correlation between fracture toughness and impact toughness. Kumar and Seal[28] in their studies on En-16 and En-19 steels found that increase in fracture toughness value results in an increase in impact energy and $(K_Q)^2$ and CVN are linearly correlated. The objection here is that they have correlated K_Q with CVN and not K_{IC}. K_Q values are not true fracture toughness values of the material but are termed as conditional fracture toughness values. K_Q is not a true material property. Therefore, the whole purpose of such studies is highly questionable.

Padmanabhan and Wood[10] in their studies on 300M steel have reported the inverse response of Charpy impact and plane strain fracture toughness to microstructural variations. CVN energy consistently dropped with an increase in K_{IC}. No difference in fracture modes of K_{IC} and CVN specimens was

observed. While the notch root radius tends to zero for the K_{IC} specimens, it was 0.25 mm for CVN specimens. The anamolous toughness behavior is explained based on this notch root radius variation. However, simultaneous improvement in both these properties was achieved by incorporating a fine grained lath martensite morphology and a fine carbide dispersion through a modified heat treatment.

In fact, there is no theoretical basis for the two parameters to have some correlation since a static fracture toughness test essentially involves a sharp crack, a thick specimen for plane strain condition, a slow rate of loading and a flat fracture mode, whereas the dynamic fracture toughness test involves a blunt notch, relatively thin specimen, a high rate of loading and a mixed mode of fracture.

A remarkable correlation exists in the constant relationship between hardness, tensile strength, yield strength, and reduction of area of quenched and tempered low alloy steels regardless of composition. Fig. 2.9[26] shows this correlation.

2.6 Embrittlement During Tempering:

High Strength martensitic steels, heat-treated to achieve optimum combinations of strength, ductility, and toughness are susceptible to embrittlement during tempering. This loss in toughness can result primarily from two types of thermal treatments.[15]:

1.   Holding or slow cooling alloy steels, previously tempered

above 600°C, in the temperature range 350 to 550°C

(Temper Embrittlement), Fig. 2.10.[26]

2. Tempering as-quenched alloy steels in the range 250

to 450°C (Tempered Martensite Embrittlement), Fig.

2.11[26].

2.6.1 Temper Embrittlement Phenomenon (TE):

There is a large body of evidence[15] linking the

phenomenon of temper embrittlement or "high temperature

embrittlement" or "two step embrittlement" to the grain boundary

weakening effect of segregated impurities or 'tramp' elements

(e.g., S,P,, Sb, Sn, etc). The fracture mode observed in this

case is found to be predominantly intergranular.

2.6.2 Tempered Martensite Embrittlement (TME):

The mechanism[15] of Tempered Martensite Embrittlement(TME),

also known as "500'F or 350°C" or "one step embrittlement"has

remained somewhat a mystery. In this case Charpy V-notch impact

energy decreases suddenly and transition temperature increases

during tempering. Fracture toughness is also seen to be degraded in

certain steels but such measurements were not always consistent

in revealing the embrittlement. Fracture modes in the

embrittlement range have been found as intergranular, cleavage,

quasi-cleavage, fibrous, mixed ductile-brittle, martensite

translath, and martensite interlath|packet etc. TME was also

found time-dependent at differing tempering temperatures,i.e.

tempering at longer times somewhat below the characteristic

embrittling temperature also resulted in embrittlement. Si and Al both these elements are known to retard the replacement of carbide by cementite to higher tempering temperatures. It was found that in such modified steels the embrittlement trough was correspondingly displaced to higher temperatures.

The mechanisms suggested for TME are summarized as follows[15]:

1. Embrittlement is concurrent with the formation of platelet cementite, replacing ε -carbide. This occurs on grain and lath boundaries. In steels where the level of impurities/retained austenite is small, the dominant embrittlement mechanism is the tensile fracture of such carbides and the resulting fracture mode will be transgranular cleavage.

2. However, the consequence of interlath carbide precipitation is mechanical destabilization of the remaining interlath austenite, resulting in largely stress-assisted transformation to an interlath layer of untempered martensite. This provides an increasingly major contribution to embrittlement in microstructures containing larger volume fractions of austenite, resulting in an interlath cleavage fracture mode.

3. In steels containing sufficient residual impurity content, such impurities, particularly P, will tend to segregate

to prior austenite grain boundaries during austenitization.
In the embrittlement range, the combination of cementite
precipitates and impurities in prior austenite grain boundaries
will lead to the lowest cohesion at grain boundary, carbide
matrix interfaces, resulting in an intergranular fracture.

TME in a given steel can not be generally attributed
to a single mechanism. All three may act in concert and the
resultant fracture mode merely indicates the weakest path.

In the recent studies carried out by Materkowski and
Krauss[19] on a low alloy SAE 4340 steel, revealed that TME was
observed for Charpy impact toughness values but plane strain
fracture toughness increases with increasing tempering
temperature, even in the TME range. A narrow zone of ductile
fracture immediately adjacent to the fatigue pre crack
accounts for the high K_{IC} values, and is attributed to the
reduced rate of work hardening in specimens tempered in the
critical range. Rapid extension of the overload crack beyond
the ductile zone produces the cleavage fracture characteristics
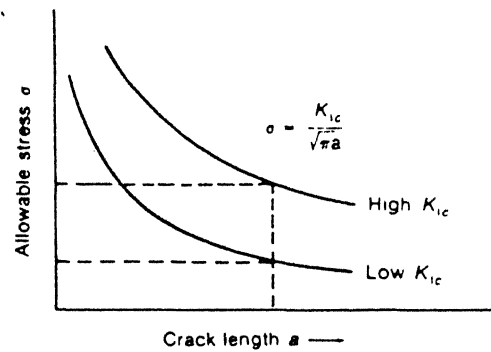of embrittled CVN specimens.

$$\sigma = \frac{K_{Ic}}{\sqrt{\pi a}}$$

Fig. 1.1   Relation between fracture toughness and allowable stress and crack
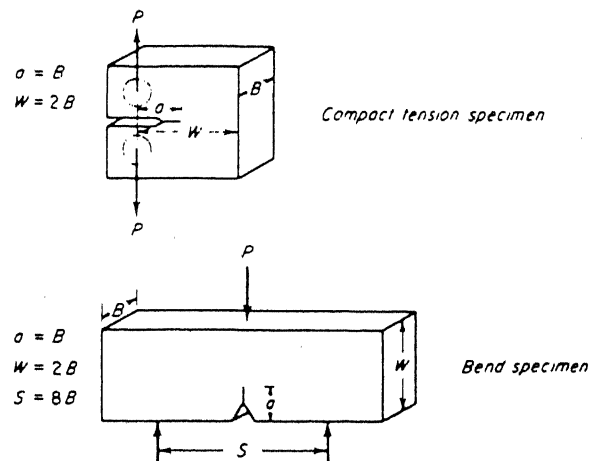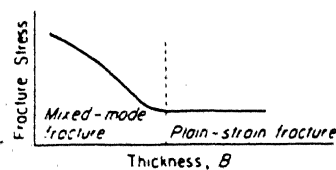

Fig. 2.1   Common specimens for K_{IC} testing

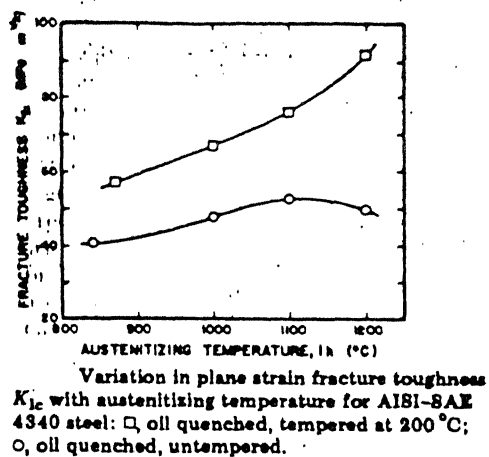Fig. 2.2   Effect of specimen thickness on fracture stress

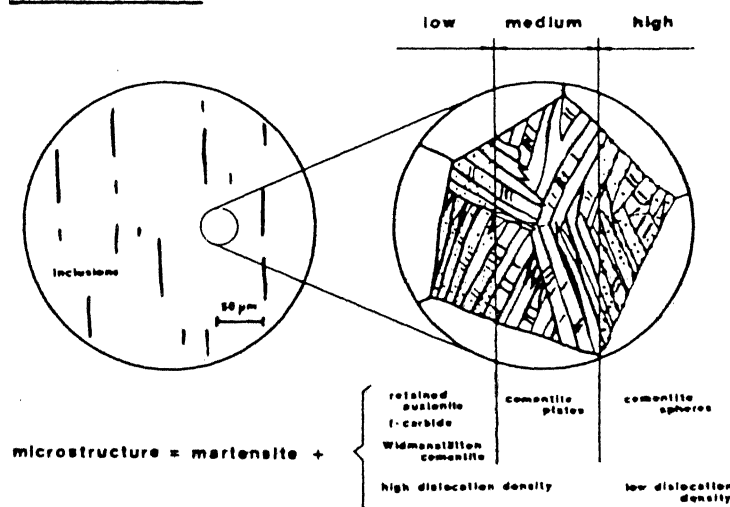Variation in plane strain fracture toughness K_{Ic} with austenitizing temperature for AISI-SAE 4340 steel: □, oil quenched, tempered at 200 °C; O, oil quenched, untempered.

Fig. 2.3

-Room temperature Charpy impact energy vs tempering temperature for 4340 steel austenitized at 1143 K (870°C), oil quenched, and tempered 1 h at temperatures shown.
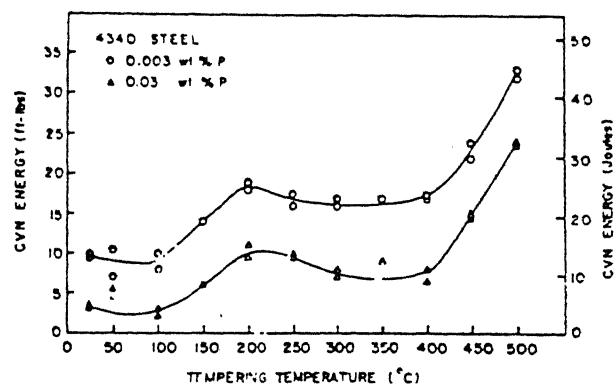
Fig. 2.4

Microstructure:

tempering temperature:

low   medium   high

microstructure = martensite +

retained austenite
ε-carbide
Widmanstätten cementite
high dislocation density

cementite plates

cementite spheres

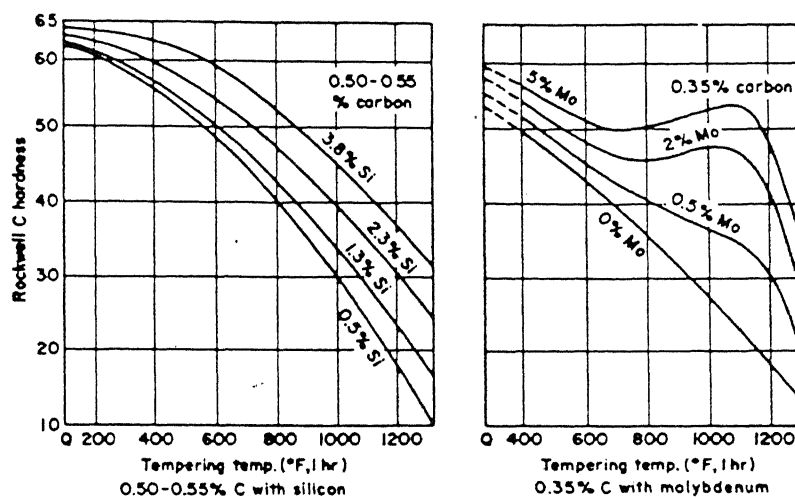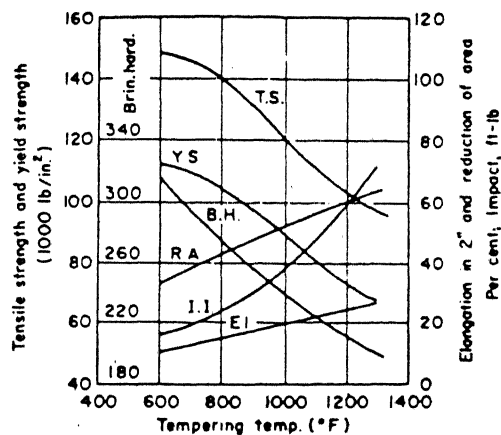low dislocation density

Possible types of microstructures depending on tempering temperature
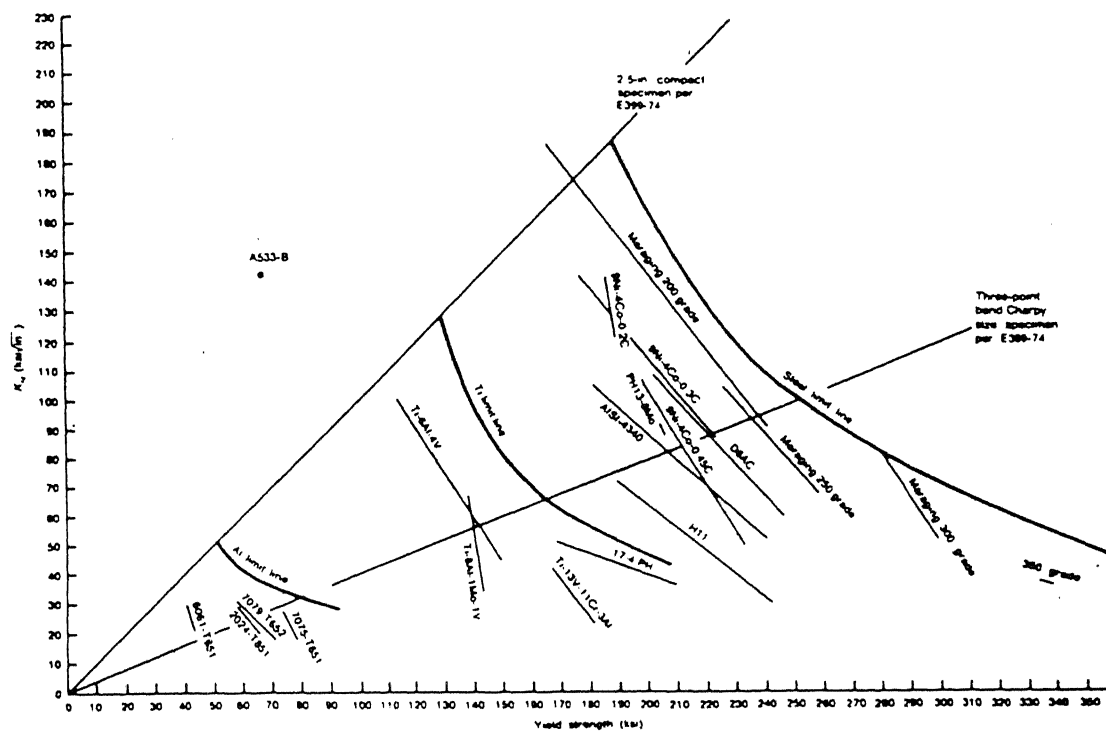
Fig. 2.5

Comparison of softening characteristics in tempering of a steel containing silicon (non-carbide-forming) with a steel containing molybdenum (carbide-forming).
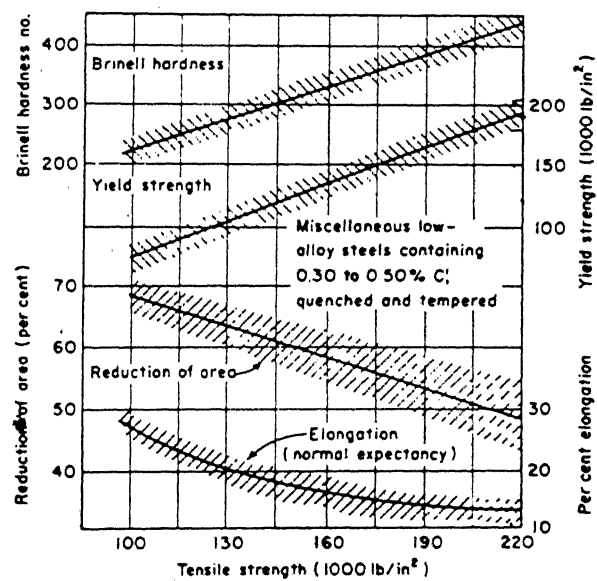
Fig. 2.6

Properties of SAE 1045 steel quenched in water from 1475-1525 F and tempered at temperatures indicated.
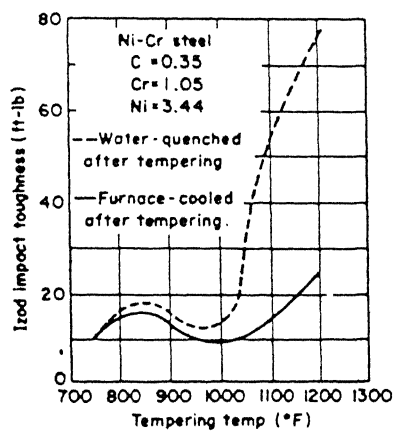
Fig. 2.7

Range of toughness and yield strength values for a variety of alloys at room temperature
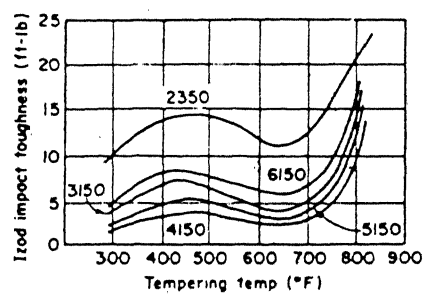
Fig. 2.8

Probable mechanical properties of tempered martensite.

Fig. 2.9

Impact toughness vs. tempering temperature for a temper-brittle steel.

Fig. 2.10

Impact toughness vs. tempering temperature for five alloy steels fully hardened before tempering.

Fig. 2.11

CHAPTER-III

EXPERIMENTAL PROCEDURE

3.1   Material

The material was supplied by Track Parts of India Limited, Kanpur. The alloy is used commercially in chain links of earthmoving equipments and other applications. Chemical composition of the alloy was as follows:

C	Mn	Si	S+P	Cr	Mo
0.33-0.37%	1.1-1.4%	0.35% max	0.05% max	0.3-0.5%	0.15%

Ingots were first rolled to 4"x4" billets and then forged. All the samples were machined out from material in forged condition.

3.2   Preparation of Test Specimens:

(a) Tensile Specimens:

Tensile samples were prepared according to the following dimensions:

Gauge length	= 20 mm
Length of grip	= 25 mm
Length of the portion joining gauge and grip	= 3 mm
Diameter in the gauge	= 6 mm
Diameter in the grip	= 9 mm
Total length of the sample	= 76 mm

The specimen is shown in Fig. 3.1 (a).

(b) <u>Charpy V-notch Specimens</u>:

Standard Charpy V-notch samples were prepared according to the following dimensions.

Length of the sample	= 58 mm
Area of cross-section	= 10 mm x 10 mm
Depth of V-notch	= 2 mm
Angle of notch	= $45°$
Notch root radius	= 0.25 mm

The specimen is shown in Fig. 3.2(b).

(c) <u>K_{IC} Specimens</u>:

The tree-point loaded bend specimen was used for plane-strain fracture toughness testing. The specimens were prepared as per ASTM standard. A suitable thickness was first chosen and accordingly other dimensions were determined. Samples of two different sizes were prepared according to following dimensions:

		<u>Small Sample</u>		<u>Big Sample</u>	
Thickness	B	16	mm	24	mm
Width	W	32	mm	48	mm
Total length	L	152	mm	200	mm
Span	S	128	mm	192	mm

Crack to width ratio $\frac{a}{w}$ = 0.45 to 0.55.

The crack length a includes both the depth of the notch and the length of the fatigue crack. Fatigue crack starter notch was machined in the sample before the heat treatment. The specimen is shown in Fig. 3.1(c).

3.3   Heat Treatment:

All prepared samples were subjected to heat treatment schedules as follows:

(i)   Tensile specimens austenitized at 870°C for 90 minutes followed by oil quenching and then tempering at 200°C, 250°C, 300°C, 400°C and 450°C for 1½ hours.

(ii)   Charpy specimens austenitized at 870°C for 90 minutes followed by oil quenching and then tempering at 200°C, 250°C, 300°C, 400°C and 450°C for 1½ hours.

(iii)   Plane-strain fracture toughness specimens austenitized at 870°C for 90 minutes followed by oil quenching and then tempering at 200°C, 250°C, 300°C and 400°C for 1½ hours.

After tempering all the samples were air cooled to room temperature.

All the heat treatments were carried out in Muffle furnaces with electronic temperature controllers. Usual Pt/Pt. Rh and chromel│alumel thermocouples were used for temperature measurements. Cast iron filings were used to cover the

samples for preventing or minimizing decarburization and oxidation of samples.

3.4 Mechanical Testing:

(a) Tensile samples were tested on Universal Testing Machine of 30 ton capacity using cross-head speed of 10^{-5}/sec.

(b) For impact toughness testing a pendulum type Charpy V-notch testing machine was used. The hammer velocity was 3.3 m/sec in accordance with the ASTM standard.

(c) K_{IC} specimens were tested using a Materials Testing System (MTS) machine of 10,000 Kg. capacity. Samples were first subjected to fatigue precracking.

$\sigma_{min}/\sigma_{max}$ ratio was kept +0.1 during fatigue precracking. If the load cycle is maintained constant, the maximum K (stress intensity) and the K range will increase with crack length. Higher K values result in undesirably high crack growth rates. Therefore both maximum and minimum loads were continuously decreased with increasing crack length keeping $\sigma_{min}/\sigma_{max}$ ratio constant. The frequency used was 15 Hz. The testing and evaluation of fracture toughness values were carried out in accordance with the ASTM standard-E399. All the fracture toughness

values were found to be valid K_{IC} values using minimum specimen thickness criterion $B = 2.5\left(\frac{K_{IC}}{\sigma_0}\right)^2$ except for the specimen tempered at $400^{\circ}C$.

(d) Hardness testing was done in a Rockwell hardness tester using C sale, i.e., diamond brale indenter and a 150-Kg major load. Samples for hardness testing were cut from broken K_{IC} specimens. A large number of readings were taken on throughout the cross-sectional area as well as on outer surface and then averaged.

3.5 Metallography:

Samples for metallographic studies were cut from broken K_{IC} specimens. Samples were ground, polished and etched. 5% nital solution was used as etchant. Alternate polishing and etching were carried out several times to remove completely distorted surface and to reveal the true structure of the specimens. All the samples were observed under optical microscope and photographs were taken.

3.6 Scanning Electron Microscopy:

Samples for fractographic studies were cut in appropriate sizes using power hack-saw from both K_{IC} and Charpy V-notch specimens. Fracture surfaces were cleaned using acetone to remove any grease or foreign particles. The test samples were then scanned at various magnifications and photographs were taken to study the mode of fracture. The operating voltage was fixed at 15 kV.

42

(a) Tensile Specimen

(b) Charpy V notch specimen

(c) K_{IC} Specimen (three point bend)

(All dimensions are in mm)

Fig. 3.1

EXPERIMENTAL RESULTS AND OBSERVATIONS

The experimental results obtained in the present investigation
for the given steel are reported as follows:

4.1 Variation of Hardness with Tempering Temperature:

Hardness values of the steel used in this investigation
for various treatments are given in the following Table 4.1.
The values reported are the average values of a large number
of readings taken for each treatment.

Table 4.1

Tempering Temperature ($^{\circ}$C)	As quenched	200	250	300	400	450
Hardness (RC)	55	50	48	45.5	40.5	38

Fig. 4.1 shows the hardness variation with tempering temperature.
The hardness decreases with increasing tempering temperature.
The hardness decreases more rapidly after tempering at 250°C,
while below this temperature the decrease is not much.

4.2 Variation of Tensile and Yield Strength with Tempering Temperature:

Tensile strength and yield strength values of the given steel for different treatments are given in the following Table 4.2.

Table 4.2

Tempering Temperature (^{o}C)	200	250	300	400	450
Yield Strength (MPa)	1630	1550	1470	1230	840
Tensile Strength (MPa)	1880	1790	1690	1400	1230

The variation of Tensile Strength and Yield Strength with tempering temperature have been shown in Fig. 4.2. Both tensile as well as yield strengths decrease with increasing tempering temperature. These vary consistently with tempering temperature.

4.3 Impact Toughness Variation with Tempering Temperature:

The Charpy V-notch Impact Toughness values for various treatments are shown in the following Table 4.3. These are

based on average of 3 specimens tested.

Table 4.3

Tempering Temperature ($^\circ$C)	As quenched	200	250	300	400	450
Impact Energy (Joules)	22.5	106.8	61.7	48.5	29.4	69.6

Fig. 4.3 shows the variation of Impact Toughness with tempering temperature. Impact toughness, in the beginning increases with tempering temperature, then starts decreasing and passing through a minimum again shows an increasing trend with increasing tempering temperature. The peak toughness is observed at a tempering temperature of 200°C while minimum occurs at 400°C. This "toughness trough" is an example of tempered martensite embrittlement (TME).

4.4 Variation of Plane-Strain Fracture Toughness (K_{IC}) with Tempering Temperature:

The results of plane-strain fracture toughness testing using a three-point bend test are shown in the following Table 4.4.

Table 4.4

Tempering Temperature ($^\circ$C)	200	250	300	400
Plane Strain Fracture Toughness K_{IC} (MPa $\sqrt{m}$)	53.5	82.0	115.0	Invalid result

The test samples tempered at $200^{\circ}C$ and $250^{\circ}C$ were of smaller
size (thickness B=16 mm). After observing the values of
fracture toughness(K_{IC}) for the given steel, the thickness
and accordingly other dimensions were increased 1½ times
of the smaller sample. However, it is to be noted that
the specimen tempered at $400^{\circ}C$ failed to meet ASTM requirements
for valid K_{IC}. Therefore, this result has not been reported.

Fig. 4.4 shows Fracture Toughness as a function of tempering
temperature. The fracture toughness increases with increasing
tempering temperature. A nearly two-fold increase has been
noted in K_{IC} on increasing tempering temperature from $200^{\circ}C$
to $300^{\circ}C$. No "toughness trough" or tempered martensite
embrittlement has been noted at least within this tempering
temperature range.

Figures 4.5, 4.6 and 4.7 show the relationship of plane-
strain fracture toughness(K_{IC}) with hardness, tensile and
yield strength and Charpy V-notch impact energy respectively
observed in the present investigation. K_{IC} is found
inversely related with hardness and strength as expected.
Almost a linear relationship has been observed. However,
K_{IC} decreases with increasing impact toughness and an
inverse relationship has been found between these two
properties for the given steel and heat-treatment conditions.

4.5 Microstructure:

Microstructures obtained for tempering temperatures of 200°C, 250°C and 300°C have been shown in Fig. 4.8.

The microstructure of the specimen tempered at 200°C essentially consists of tempered martensitic structure with a small amount of retained austenite. The martensite at this carbon content is predominantly of lath type but some martensite needles are also visible. The microstructures at 250°C and 300°C do not exhibit retained austenite at all. In this temperature range the retained austenite perhaps decomposes into bainite. The amount of carbide particles precipitated increases at 300°C.

4.6 Fractography:

Some of the representative scanning electron fractographs of steel samples treated at different temperatures and under different modes of loading are shown in Fig. 4.9-4.11. Fig. 4.9 shows the fractographs of Charpy specimens. All the fractographs show the basic fracture mode as of quasicleavage type. At 200°C the fracture of more ductile nature with a few flat facets. More and more flat quasicleavage facets and decrease in ductile features are observed as tempering temperature reaches to 300°C. The size of the facets also increases.

Fig. 4.10 shows the fractographs of K_{IC} specimens at two different magnifications. The fractographs again show the basic mechanism of fracture as quasi-cleavage. The fractographs of the specimens tempered at $300^{\circ}C$ exhibit more ductile features as compared to those tempered at $200^{\circ}C$.

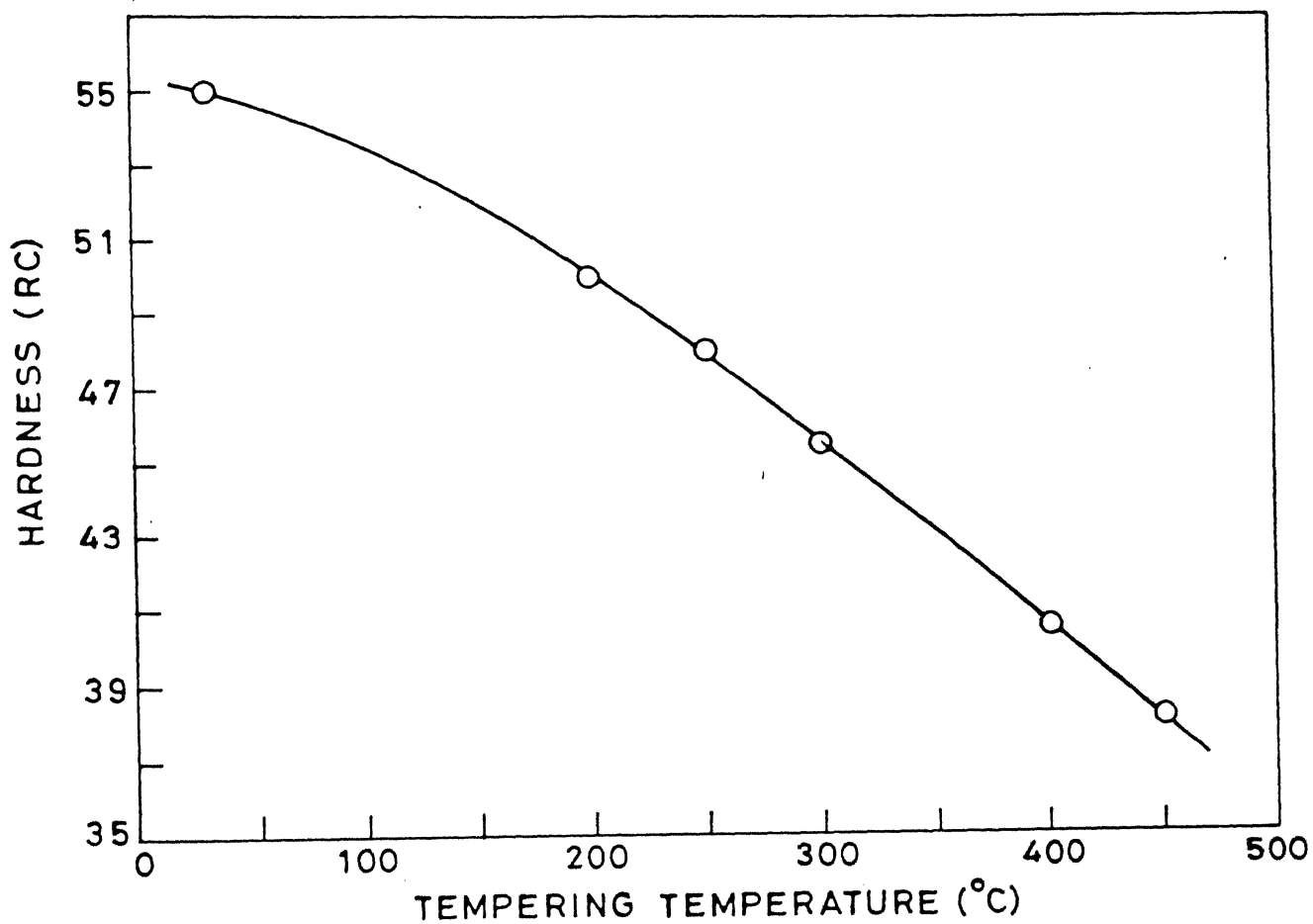Fig. 4.11 shows the fractographs of interface of fatigue precrack and overload fracture zone in K_{IC} specimens.
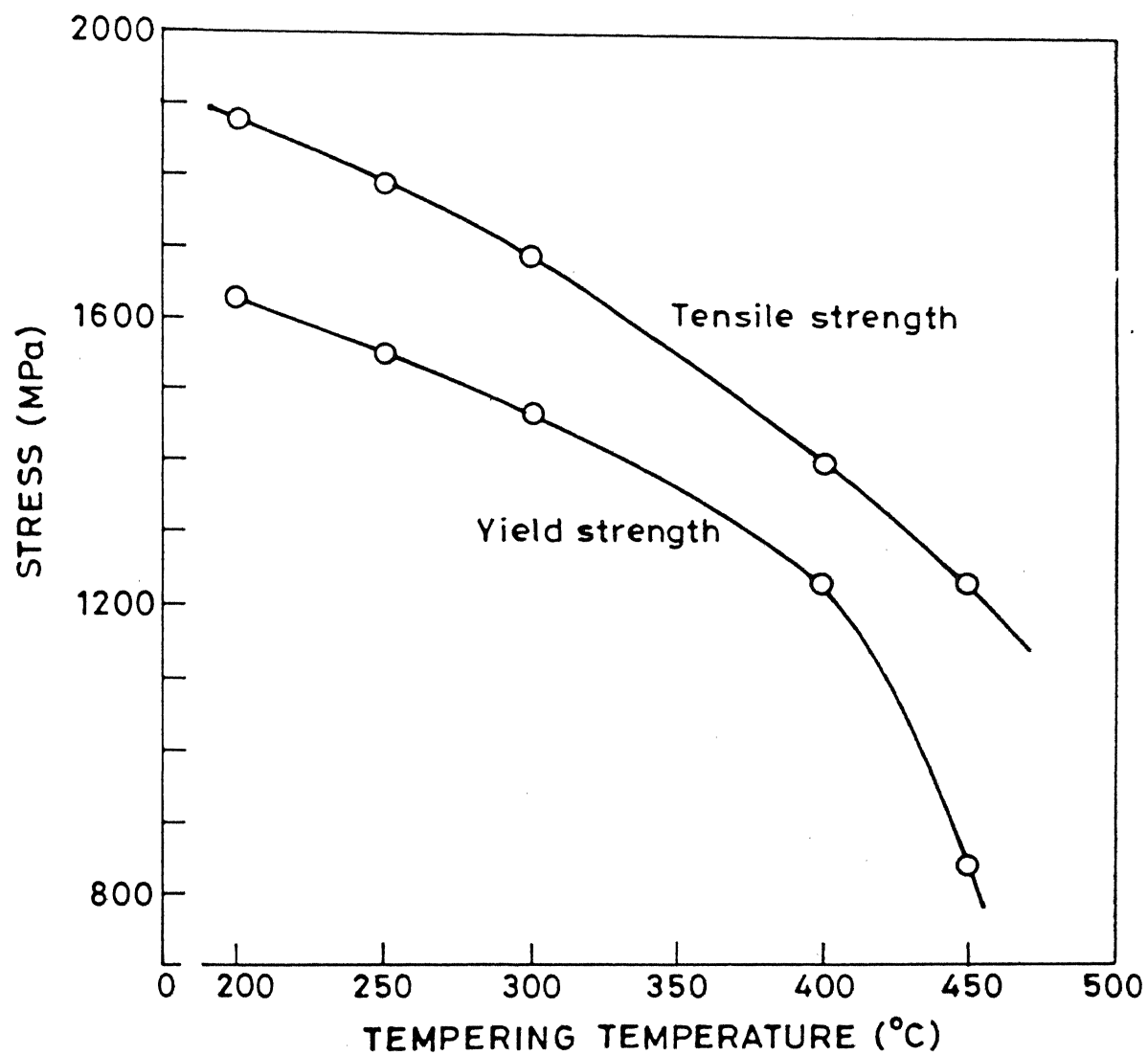
Fig.4.1 Hardness as a function of tempering temperature.

Fig. 4.2 Tensile strength and yield strength as a function of tempering temperature.
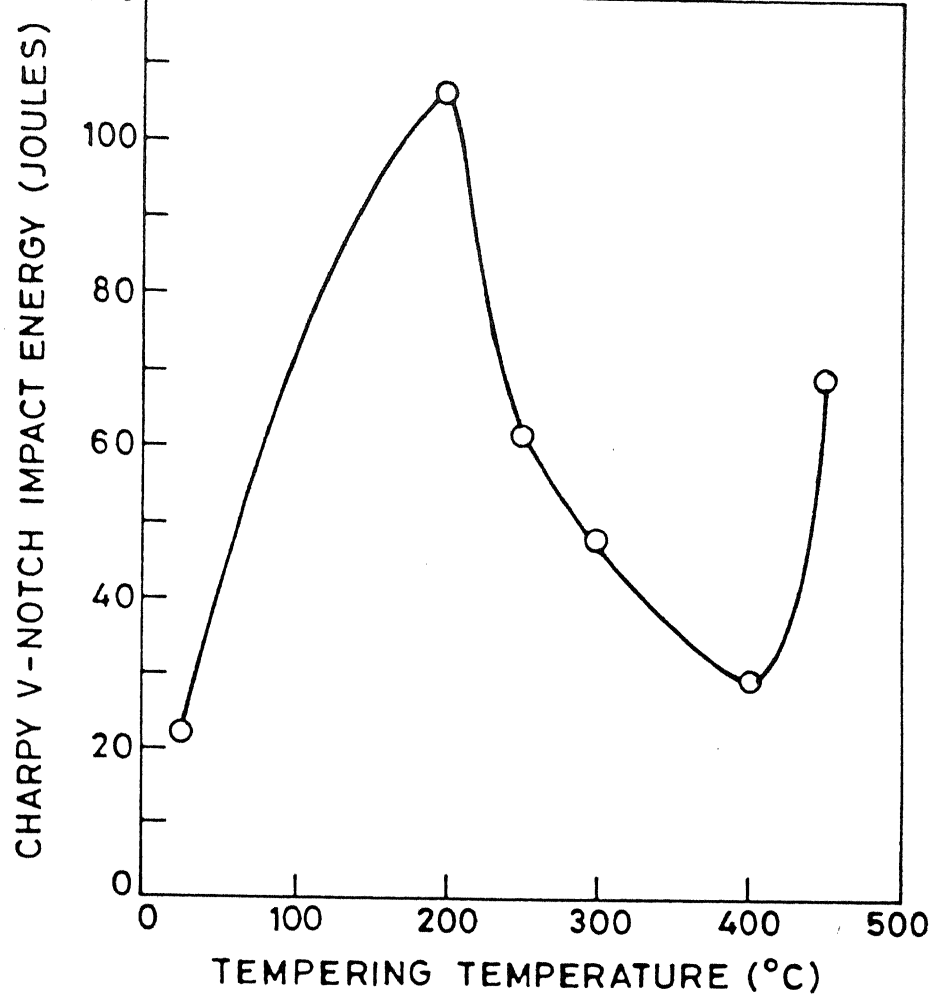
Fig. 4.3 Impact toughness as a function of tempering temperature.
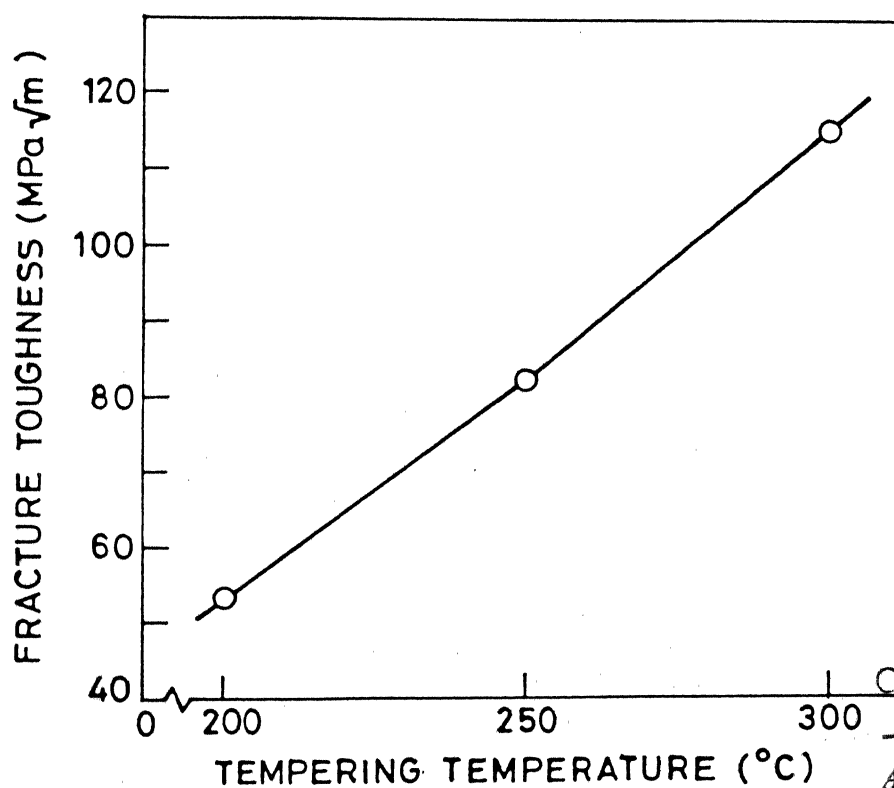
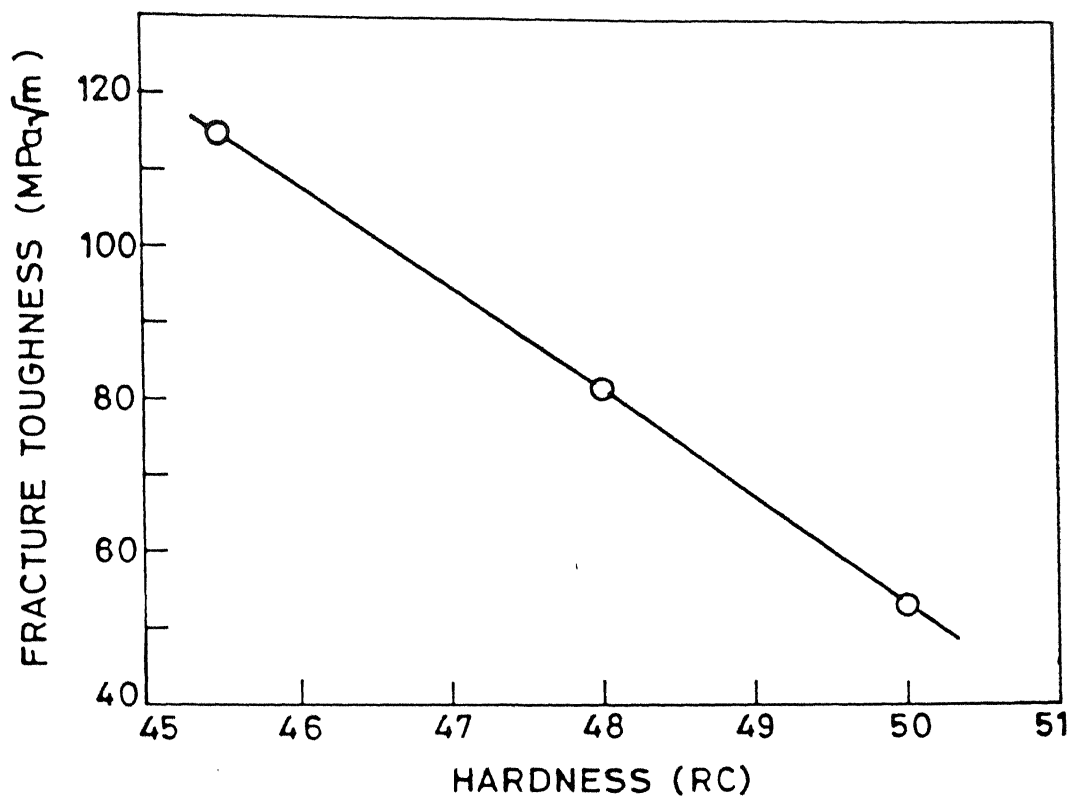Fig. 4.4 Fracture toughness as a function of tempering temp.

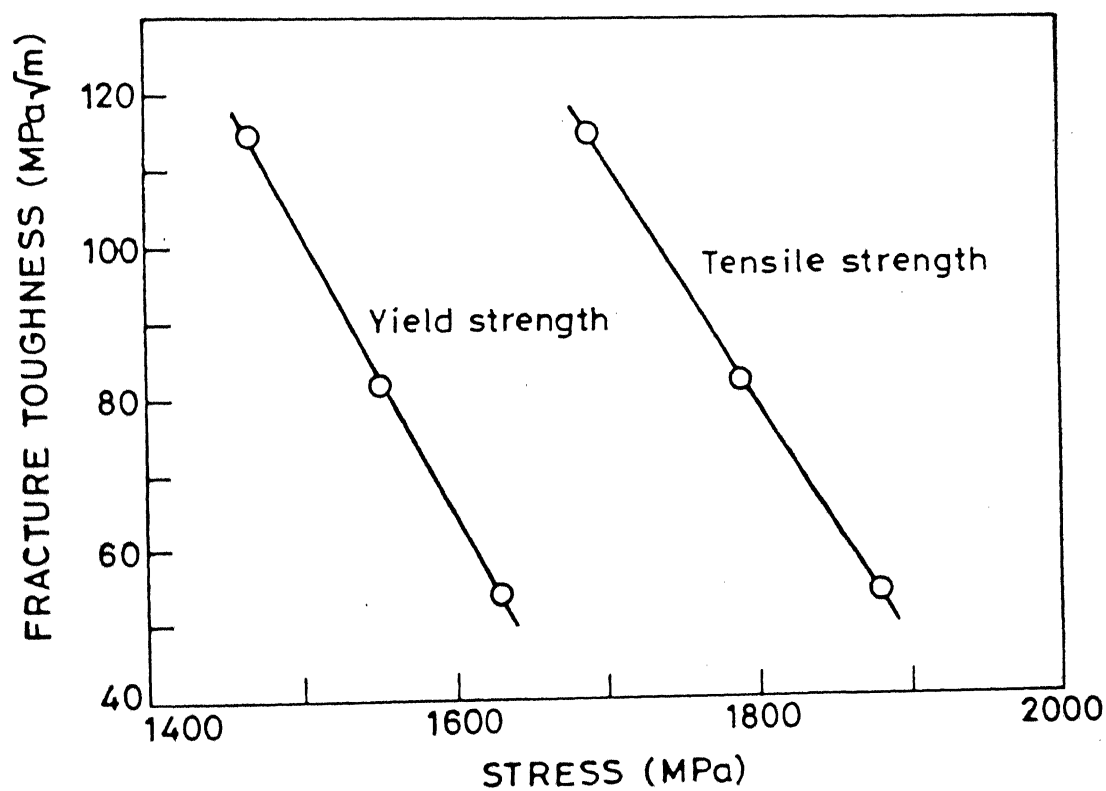Fig. 4.5 Relationship between hardness and fracture toughness

Fig. 4.6 Relationship between yield strength and fracture tough-
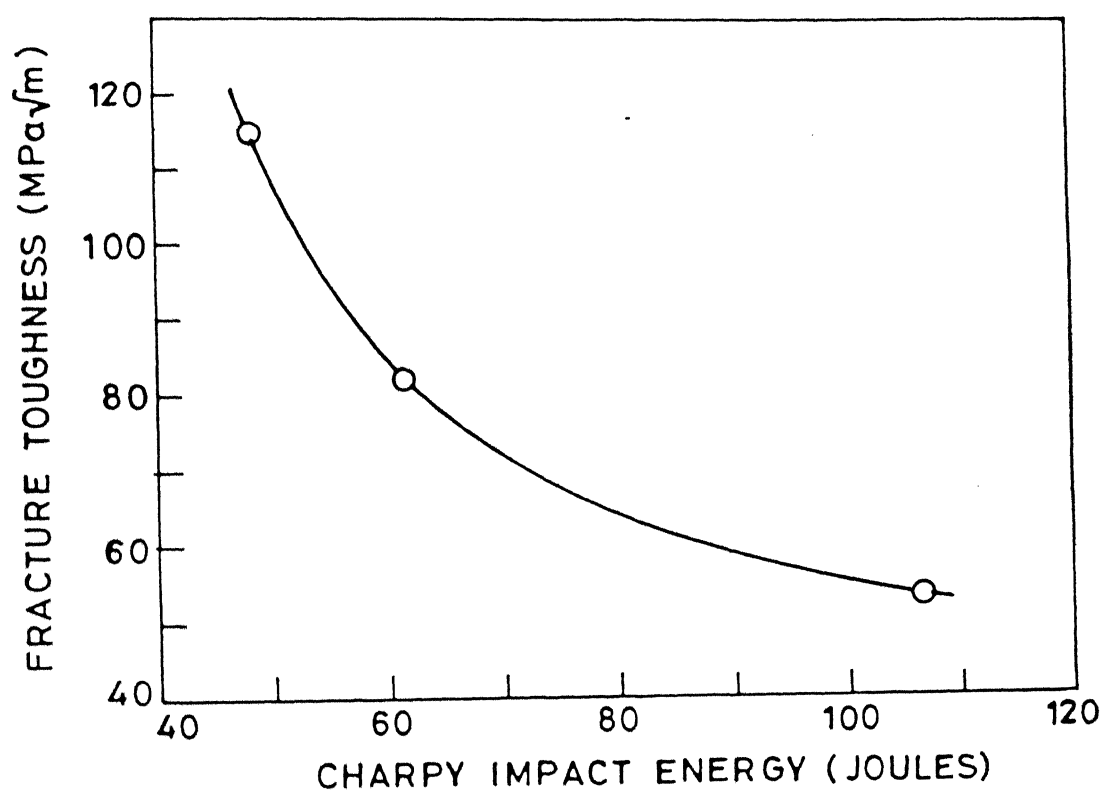ness and tensile strength and fracture toughness.
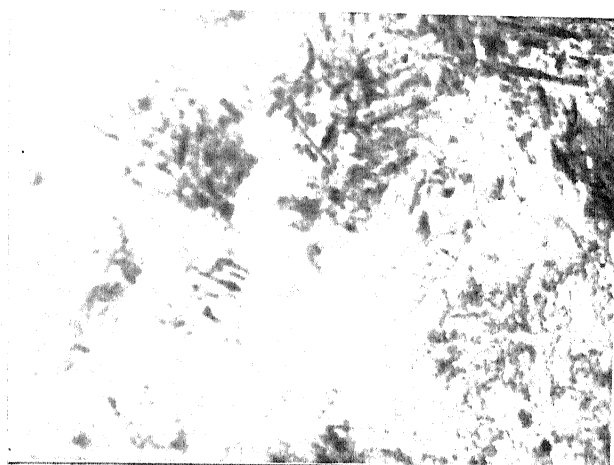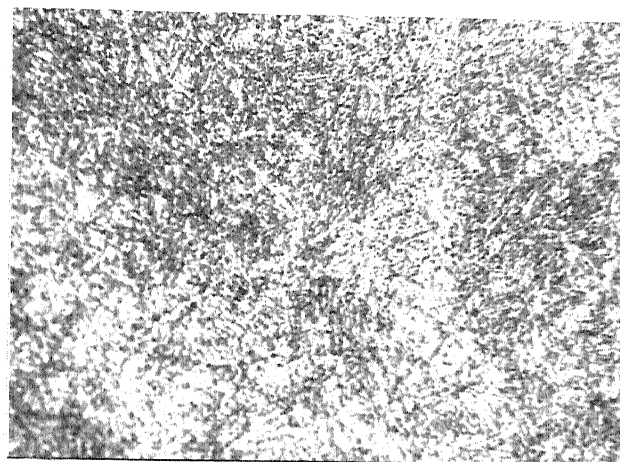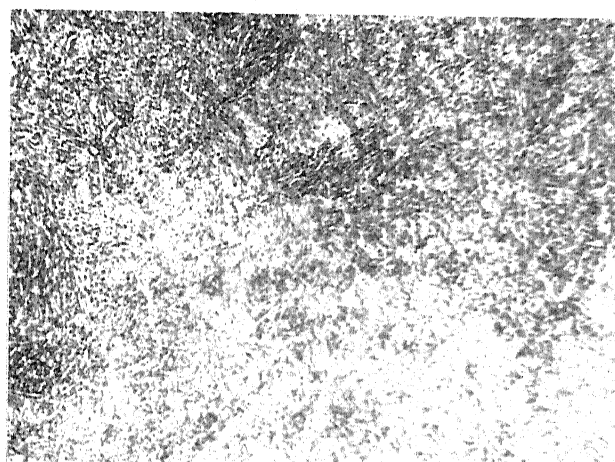
Fig. 4.7 Relationship between impact toughness and fracture toughness.

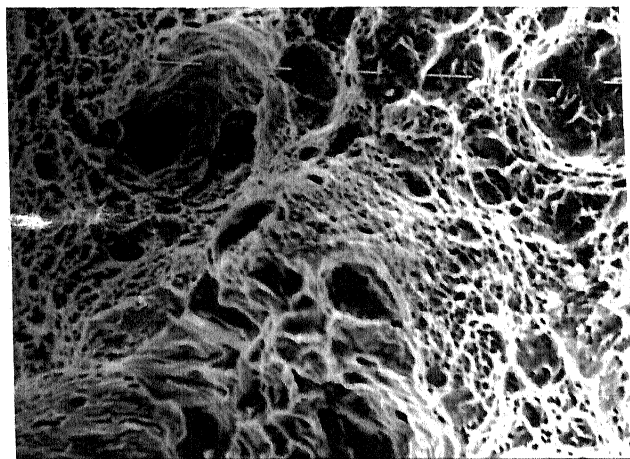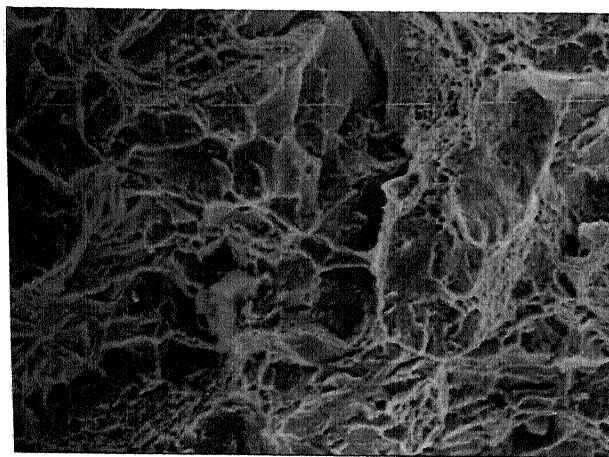(a)   Mag. 1500X   (b) Mag. 1500X

(c) Mag. 1500X

Fig. 4.8   Microstructures of the steel specimens
             austenitized at 870°C for 1½ hours,
             oil quenched and tempered at (a) 200°C
             (b) 250°C and (c) 300°C for 1½ hours

(a) Mag. 4000X   (b)   Mag. 4000X
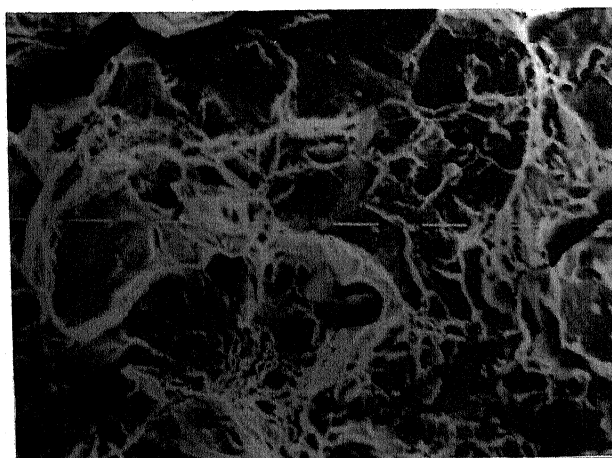
(c) Mag. 4000X

Fig. 4.9   Scanning Electron Fractographs of CVN steel
           specimens austenitized at 870°C for 1½
           hours, oil quenched and tempered at (a) 200°C
           (b) 250°C and (c) 300°C for 1½ hours
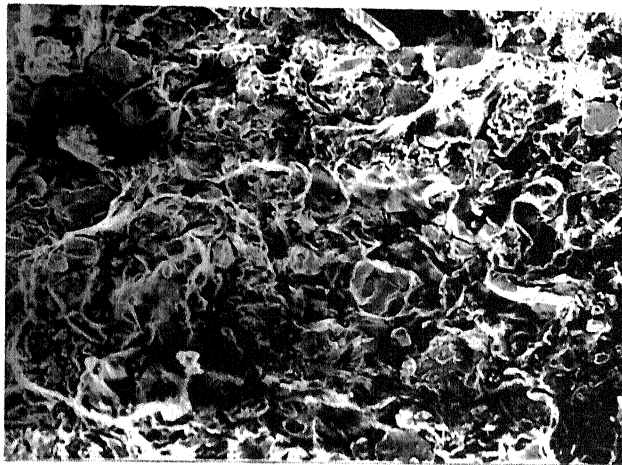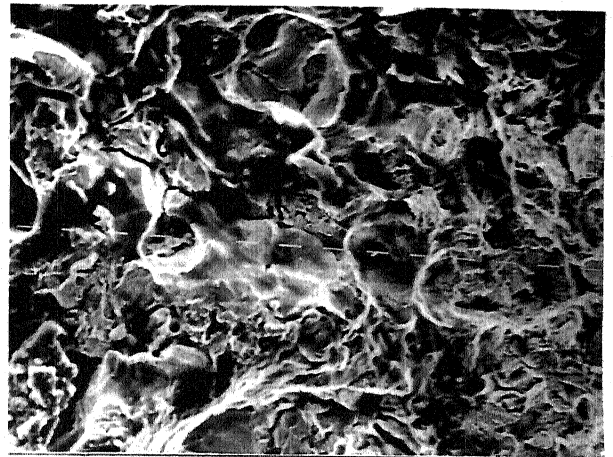
(a)   Mag. 600X   (b)   Mag. 2500X
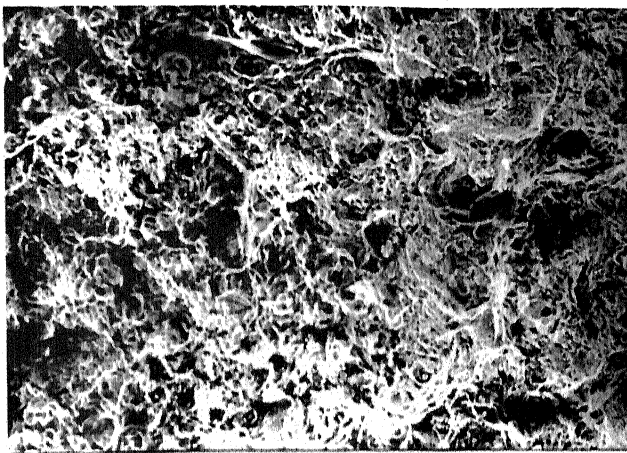
(c)   Mag. 600X   (d)   Mag. 2500X

Fig. 4.10   Scanning Electron Fractographs of K_{IC} specimens
austenitized at $870^{\circ}C$ for $1\frac{1}{2}$ hours, oil
quenched and tempered at $200^{\circ}C$(a) and (b)
and at $300^{\circ}C$ (c) and (d) for $1\frac{1}{2}$ hours.
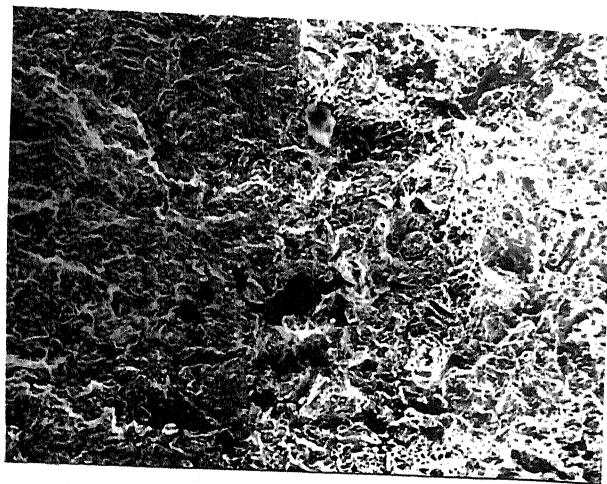
(a)   Mag. 600X
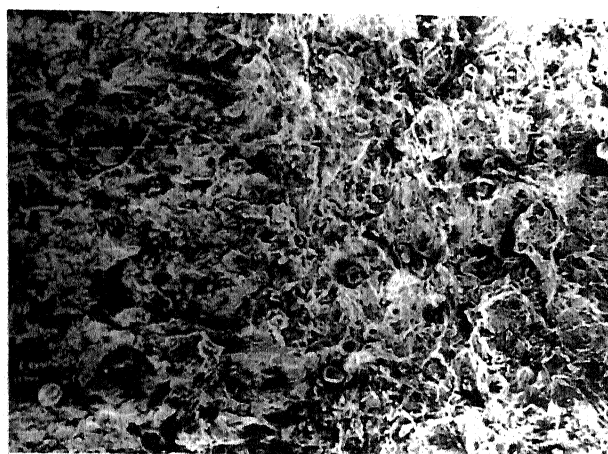
(b)   Mag. 600X

Fig. 4.11   Scanning Electron Fractographs of interface
of fatigue precrack and overload fracture
zone in KIC specimens austenitized at 870°C
for 1½ hours, oil quenched and tempered at
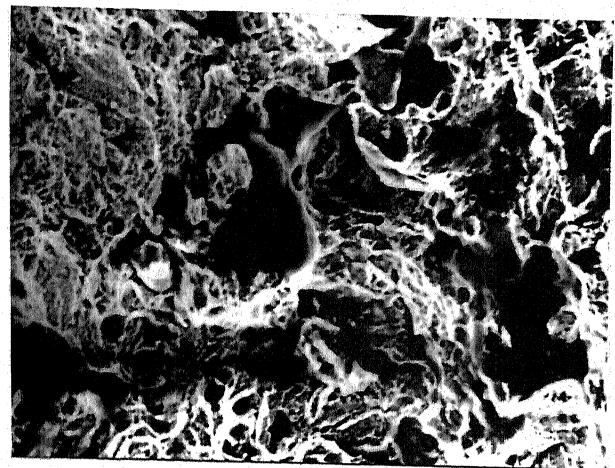(a) 250°C and (b) 300°C for 1½ hours.
Interface bisecting micrograph from top to
bottom, fatigue precrack (right) and
overload (left).

CHAPTER-V

DISCUSSION

Various results obtained in the investigation are
discussed in this chapter.

5.1 Hardness Behavior:

Decrease in hardness with increasing tempering
temperature is in perfect agreement with the well-known
trend of hardness vs. tempering temperature. While
the precipitation of ε carbide from the martensite matrix
contributes a softening component. The observed hardness
is, therefore, a net result of these two effects. The
decrease in hardness becomes more appreciable after tempering
at 250°C. This may be attributed to the fact that a small
amount of retained austenite is present below this
temperature. The retained austenite when converted to
bainite upon tempering contributes a hardening effect and
increases resistance to softening upon tempering in this
temperature range.

5.2 Tensile Behavior:

Tensile strength and yield strength both decrease
with increasing tempering temperature. As hardness varies
directly with ultimate tensile strength this is in agreement

with the theoretical results and the structures obtained.
At higher and higher tempering temperatures the martensite
is more and more depleted in carbon resulting in decrease
in its tetragonality and hence the strength goes down.
Decrease in strength is more pronounced with higher and
higher tempering temperatures when martensite decomposes
to ferrite and carbide phases.

5.3   Impact Toughness Behavior:

Impact toughness of the steel under investigation
initially rises, then decreases and again rises. This is
in confirmity with the general observations made on
medium carbon heat treatable steels. The initial rise in
toughness is explained in terms of elimination of internal
stresses arising out of rapid cooling during quenching and
loss of tetragonality of martensite due to precipitation
of a coherent phase: viz ε carbide.

As the tempering temperature is increased beyond
$200^{\circ}C$, carbide phase is nucleated at the lath boundaries
and the original austenite grain boundaries. The carbides
are essentially incoherent and they tend to form a plate-
like structure which influences easy crack nucleation and
its propagation. With the increasing temperature of
tempering the carbide platelets grow and further decrease
the toughness. Eventually, the carbides tend to coalesce

in a spherical geometry and thus decrease their detrimental effect on the crack propagation phenomenon. At this stage toughness starts increasing again. With the spheroidization process increasing with higher temperatures the toughness keeps on increasing.

The phenomenon of tempered martensite embrittlement has also been related to segregation of impurities at prior austenite grain boundaries and mechanical destabilization of retained interlath austenite. It is difficult to correlate TME with a single mechanism and in fact all of the three mechanisms may act together. The decrease in toughness value from $200^{\circ}C$ is in well agreement with the fracture modes observed. As the amount of cleavage fracture increases as shown in the fractographs the impact toughness drops. More and more cleavage facets are observed as the tempering temperature is raised.

5.4 Plane-Strain Fracture Toughness Behavior:

The most interesting results obtained in the present investigation are the variation of K_{IC} with tempering temperature and its inverse relationship with Charpy impact energy in the tempering temperature range from 200 to $300^{\circ}C$. A rapid increase in K_{IC} results as the tempering temperature is raised. The microstructure of steel sample tempered at $200^{\circ}C$ contains a finite amount of retained

austenite. The low value of K_{IC} at this temperature may be attributed to the fact that the retained austenite is perhaps mechanically unstable and decomposes into interlath untempered martensite films during slow rate of loading. Subsequent microstructures do not show the unstable retained austenite. The fracture modes as shown in Fig. 4.10 of all K_{IC} specimens are essentially of quasi-cleavage type. The quasi-cleavage facets are more clear in the sample tempered at 200°C while fracture surface shows more ductile rupture type of fracture with some quasi-cleavage facets in the specimen tempered at 300°C.

It is very significant to note that while toughness trough occurs after tempering at 200°C in case of Charpy impact tests, it is missing in K_{IC} tests. While the Charpy impact energy values drop in this temperature range, K_{IC} increases significantly with tempering temperature. Toughness troughs have also been reported for K_{IC} testing with tempering temperature for certain steels[15] between 200°C to 400°C. But only a small drop in K_{IC} has been observed in most of the cases. Other workers[10,19] have observed the absence of embrittlement during K_{IC} testing with tempering temperature and the inverse relationship between these two properties. Similar results as found in the present investigation have been reported by Materkowski and Krauss[19] on a low P SAE 4340 steel. They observed TME for Charpy impact toughness values but plane strain fracture toughness

increases with increasing tempering temperature. The
anamolous K_{IC} results have been explained on the basis of
a narrow zone of ductile fracture immediately adjacent to
the fatigue precrack. They have attributed the ductile
transition zone to the lowered rate of work hardening
and the associated ease of dislocation motion in specimens
tempered at higher temperatures as compared to the lower
tempering temperature specimens. Once rapid crack
propagation has developed, the fracture reverts to the
brittle mode observed away from the transition zone. Since
the K_{IC} values are based on the first stages of extension
of the sharp fatigue crack, the ductile fracture zone
accounts for the high measured fracture toughness. In our
present investigation no such ductile transition zone has
been observed. Fig. 4.11 clearly shows the interface of
fatigue precrack and overload fracture zone in K_{IC} specimens.
Therefore this can not be the probable reason for the absence
of toughness trough in K_{IC} test results in the present
investigation. On the basis of structural changes that are
involved to explain the drop in impact toughness of the
steel it is expected that there would be a corresponding
drop in the fracture toughness also. However, contrary to
the expectations there is no drop. The possible explanation
for the result is perhaps related to the rate of loading.
The Charpy impact test is carried out under very rapid rate
of loading while plane-strain fracture toughness test is

essentially a test under slow rate of loading. It is well known that rapid strain rates enhance the yield strength of a ductile material and decrease its total ductility. Hence under rapid loading obtained in Charpy test the steel responds in a brittle manner.

Padmanabhan et al[10] have offered an explanation for the differences in impact toughness and fracture toughness in terms of the differences in the root radius of notch in the two types of tests. Where as the Charpy specimen has a root radius of 0.25 mm, the root radius of a standard fracture toughness specimen tends to be zero. We do not agree with this explanation because propagation of a relatively blunt crack is slower than that of a sharp crack. Hence the explanation for the differences in two types of toughness must lie in the response of materials to slow and rapid rates of loading.

To have an in depth sight in the behavior of K_{IC} with tempering temperature for the present given steel one needs K_{IC} testing for the whole range of tempering temperatures. But as found in the present case beyond a tempering temperature of $300^{\circ}C$ because of the decrease in yield strength and increase in toughness the thickness of the K_{IC} specimens for valid K_{IC} testing becomes significantly high and accordingly other dimensions also. This might create problems in subsequent heat treatments. Full hardening may not occur and the structure will not be homogeneous.

The fracture toughness has also been found inversely related with hardness, yield and tensile strength . This is in the perfect agreement with most earlier findings and theoretical predictions. It is very interesting to note that for the given steel and in the tempering temperature range studied K_{IC} has almost linear relationship with hardness, tensile strength and yield strength. Similar results have been observed in one earlier investigation[28] on two commercially important En-16 and En-19 steels.

This steel is widely used in hardened and tempered conditions in critical applications when strength and fracture toughness are the two most important design parameters. The inverse relationship between the two dictates a design criterion where the product of strength and toughness should be maximum. A consideration of the product of yield strength and K_{IC} values suggests that tempering at 300°C give maximum value. Lower tempering temperature greatly decreases the K_{IC} value while the corresponding increase in yield strength is not much. Hence, tempering at 300°C yielded optimum properties in this steel.

CHAPTER-VI

CONCLUSIONS

The following conclusions are drawn from the present investigation on the AISI 4135 medium carbon low alloy steel:

1. Tempered martensite embrittlement, as documented by a plateau or trough, has been observed in CVN toughness in the temperature range from $200^{\circ}C$ to $400^{\circ}C$.

2. Plane strain fracture toughness of the present steel increases with increasing tempering temperature, even in the TME range. No toughness trough has been observed.

3. Static fracture toughness values (K_{IC}) are inversely related to dynamic fracture toughness values expressed in Charpy impact energy.

4. Fracture toughness is a complex mechanical parameter and is related to a number of basic properties other than microstructure. The difference in the rate of loading in two kinds of toughness measurements is perhaps the main factor for the anamolous toughness behavior observed in the present investigation.

5.   The fracture toughness values are inversely related to
        yield strength, ultimate tensile strength and hardness.
        A linear relationship has been observed for all these
        cases.

6.   Tempering at 300°C exhibits the best combination
        of strength and toughness in the steel under
        investigation.

        In addition, the following general conclusion on
the nature of TME can be made:

        The essential feature of TME is the precipitation
        during tempering of brittle comentite on grain and
        lath boundaries. Lath boundaries may also contain
        layers of mechanically unstable austenite, as a
        consequence of this carbide precipitation whereas
        grain boundaries may also contain residual impurity
        elements, as a consequence of segregation during
        austenitization.

REFERENCES

1. ASTM Standards Pt. 31, Designation E23-82.

2. G.E. Dieter, Mechanical Metallurgy, Third Edition, McGraw-Hill Book Company, 1986.

3. Annual Book of ASTM Standards, Vol. 03.01, Metal Test Methods, Designation E399-707.

4. R.F. Decker, Met.Trans. A, 1973, Vol. 4A, PP. 2508-2611.

5. K.H. Schwalbe, Engg. Fract. Mech., 1977, Vol. 9, PP.795-832.

6. F.A. Johnson and J.C. Radon, Int. J. Fract. Mech., 1972, Vol. 8, PP. 21-35.

7. F.M. Beremin, Met. Trans.A, 1981, Vol. 12A, P. 723.

8. R.J. Weiner, W.L. Phillips and C. Kim, Scr. Metall., 1979, Vol. 13, PP. 389-392.

9. T. Maki,S. Shimooka, M. Umemoto and I. Tamura, Met. Trans. A, 1971, Vol. 2A, P. 2944.

10. R. Padmanabhan and W.E. Wood, The Proceedings of the 4th European Conference on Fracture, Leoben, 1982, Vol. 1,PP. 264-271.

11. C.Musial and R.Brook, Engg. Fract. Mech., 1977, Vol. 9, PP.379-387.

12. J.R. Strife and D.E. Passoja, Met. Trans. A, 1978,Vol. 9A, PP. 1341-1350.

13. A.N. Kumar and A.K. Seal, Trans. IIM, 1984, Vol. 37, PP. 127-133.

14. T. Goldenberg, T.D. Lee and J.P. Hirth, Met. Trans. A, 1978, Vol. 9A,PP. 1663-1671.

15. R.M. Horn and R.O. Ritchie, Met. Trans. A, 1978, Vol. 9A, PP. 1039-1053.